NUMERICAL STUDY OF THE SHORT-TERM CLIMATIC OSCILLATION FORCED BY EL NINO DURING NORTHERN WINTER

Ni Yunqi (倪允琪), *Lin Wuyin* (林武银) and *Ning Dongmei* (宁冬梅)

Department of Atmospheric Sciences, Nanjing University, Nanjing

Received November 28, 1989

ABSTRACT

Using a nine-layer global spectral model, numerical schemes with two different SST distributions in January (control case and abnormal case) have been tested to study the climatic effect, propagation charateristics and the maintenance mechanism of the short-term climatic oscillation caused by El Nino during northern winter. The main results are as follows: (1) During northern winter, there exist two wave trains because of the influence of El Nino. One is similar to PNA pattern, and the other is similar to EUP pattern. (2) The PNA-like wave train caused by the anomalous SST forcing in central and eastern equatorial Pacific Ocean is due to the response of ultralong wave and long wave components of Rossby mode, and the EUP-like wave train crossing Eurasia is mainly due to the wave component of Rossby mode. (3) During northern winter, the warm water region in central equatorial Pacific Ocean is the source of forced wave trains. (4) In northern winter, the energy source for maintaining the short-term climatic oscillation is from the interaction between eddies, and between eddy and zonal flow.

I. INTRODUCTION

In recent years,more attention has been paid to the study of short-term climatic oscillation caused by the anomalous SST (sea surface temperature) in central-eastern equatorial Pacific during the El Nino period. Horel and Wallace (1981) first pointed out that, during ENSO periods, in northern winter the atmospheric response to the equatorial heat source may cause equivalent barotropic stationary wave trains across the Pacific and Northern America. Shukla and Wallace (1983), and Geisler et al. (1985) have experimented the atmospheric response to the equatorial SST anomaly with GCM (general circulation model), and have simulated the wave trains simillar to PNA (Pacific and North American) pattern in northern winter. According to the theory of Hoskins and Karoly (1981), the cause of these wave trains is recognized as the direct forcing of the anomalous SST in central equatorial pacific. But the GCM experiment of Geisler et al. (1985) indicated that it is inappropriate to regard the formation of the PNA pattern wave trains as the result of the direct forcing of heat source in central Pacific. They experimented with the tropical SSTA (SST anomaly) located in different longitudes, and their results showed there was not apparent change in longitude position of the mid-latitude response. Their viewpoint was also suported by Palmer and Mansfield (1986) after comparing two different GCM results. Simmons et al. (1983) found that under some conditions, the interaction between tropical forced waves and climatic stationary waves may cause stable or weak unstable normal modes, whose existence is owing to the asymmetry of the climatic mean basic flow. The idea of Simmons et al. (1983) has been verified by Branstator (1985) who pointed out that the latent heat in western Pacific and Indian Ocean decreases when SSTA is placed in central-eastern Pacific, and the atmospheric response over northern Pacific and Northern America to the anomalous heating in the areas of Indonesia and Indian Ocean is sensitive. Therefore, the Rossby wave trains can be explained as the first approximation of the atmospheric linear response to the decrease of heating. However, when they studied the midlatitude atmospheric response with the barotropic model, Held and Kang (1987) found that midlatitude wave trains formed by the forcing over central Pacific rather than western Pacific and the anomalies of divergence in extratropical zone are more important than those in tropical zone. The above studies clearly show that there exist two main problems so far in the study of atmospheric response to El Nino in extratropical zone: (1) which area is the source located——central Pacific or western Pacific? (2) What is the mechanism causing extratropical response? For understanding these two main problems, Ni et al. (1989) investigated the characteristics and mechanism of the atmospheric response to El Nino in northern summer, and their results showed that in northern summer, the source region of the extratropical atmospheric response to El Nino with time scale less than 10 days is located in the anomalous SST areas over central-eastern equatorial Pacific, and that with time scale larger than 10 days is in the western equatorial Pacific. They also suggested that the nonlinear interactions between eddy and zonal flow, and between eddies are the main mechanism for the development and maintenance of the wave trains forced by heating.Now, the problem is whether this result is also appropriate to that in northern winter, since the basic zonal flow has different structures between northern winter and summer. Therefore, in this paper attempt is made to use the same model described by Ni et al. (1989) to simulate the atmospheric response to the anomalous SST in central-eastern equatorial Pacific in northern winter, with a view to further studying the characteristics of the short-term climatic oscillation and its propagation mechanism during El Nino period. The model and the experiment scheme are described in Section II, the global climatic oscillation with the monthly time scale during El Nino period in northern winter in Section III, the dynamical characteristics of the thermally forced short-term climatic oscillation and its horizontal structure in northern winter in Section IV, and the maintenance mechanism of the short-term oscllation in northern winter is discussed in Section V. The last section gives the conclusion.

II. BRIEF DESCRIPTION OF THE MODEL AND EXPERIMENT SCHEMES

In this study, the global spectral model used cast on the sigma coordinate in vertical with nine layers from the surface to top of the atmosphere. The basic dynamic and thermodynamic equations of the model consist of vorticity equation, horizontal divergence equation, continuity equation whose surface pressure can be given after integration of the equation,thermodynamic equation and moisture tendency equation. The rohmbodal truncation is used at wavenumber 15, and the model is integrated by using the Galerkin method and the semi-implicit time integration scheme with a time step of 30 minutes.

In the model, the physical process and parameterizations include short-wave radiation, long–wave radiation,large scale condensation and convection,vertical diffusions of momentum, heat and moisture, and the effect of the underlying surface (including ocean, polar ice and snow cover) and topography on the model atmosphere are considered. More details of this model has been described by McAvancy and Bourke (1978).

In this study, the different experimental schemes are tested and the results are comparatively studied.

Scheme 1, control case (hereafter referenced "Exp 1"). SST used in the model is climatological mean values in January, and the altitude angle of the sun is in mid-January.

Scheme 2, anomalous case (hereafter referenced "Exp 2"). SST used in the model is that idealized positive SSTA which is the same as that in Lin and Sun (1987) and in Ni et al. (1989) over central-eastern Pacific superposed upon the climatological mean SST field in January. The maximum SSTA is 4.4°C. Others in the model are the same as Exp 1.

The model was integrated for 492 days from rest atmosphere, and then the two schemes were continually run for 60 days with simulation at day 492 as initialization and the January monthly average simulated results are obtained from the last 30 day averaged simulations of the experiments, respectively.

III. GLOBAL CLIMATIC EFFECT OF EL NINO WITH THE MONTHLY TIME SCALE IN NORTHERN WINTER

The simulating ability of the numerical model used here has been discussed detailedly in Lin and Sun (1987), and the results show that the model could simulate the basic characteristics of the atmospheric circulation being well consistent with those observed and exhibit strong simulating ability. In this paper, we do not describe it again, only concentrate on discussing the global climatic effect of El Nino in northern winter.

1. *Difference Field of Geopotential Height (Exp 2 − Exp 1, same in the following)*

Figs. 1a and 1b show the geopotential height difference fields at 300hPa and 850hPa (Exp 2 minus Exp1).

Fig. 1a shows that there exists significant difference center distributions bearing considerable resemblance to PNA teleconnection pattern over Pacific and northern America in upper troposphere in the Northern Hemisphere. The difference field over tropical Pacific is negative, over western coast of northern America is positive and over Mexico Gulf and Atlantic is negative. This result clearly reflects that the atmospheric response to the positive SSTA over central-eastern equatorial Pacific in the Northern Hemisphere generates PNA-like geopotential height field. Over Eurasian continent, over southern Europe and Mediterranean areas the difference field is negative, and it is positive over central Asia continent and negative over

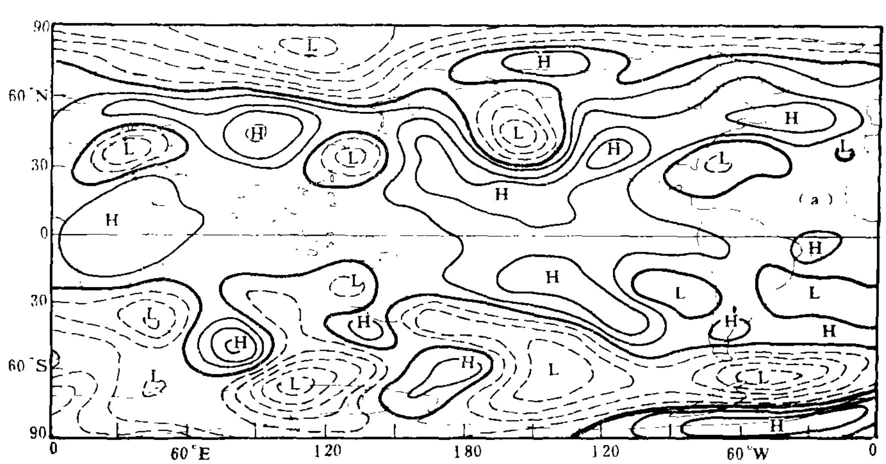

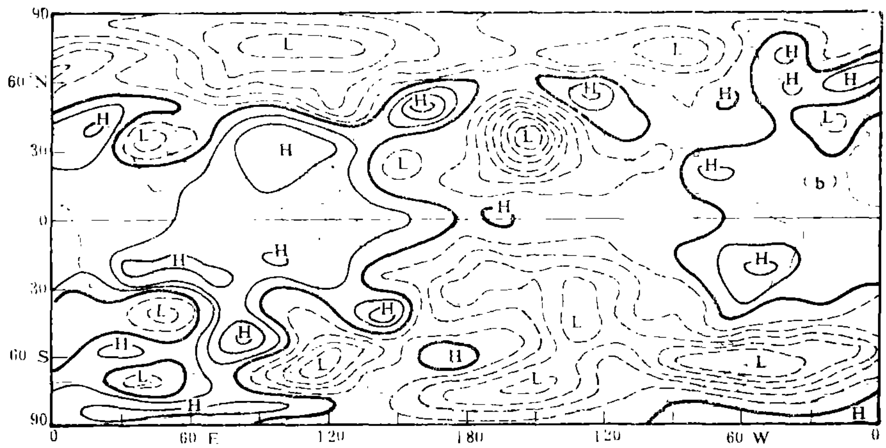

Fig. 1. Geopotential height difference field between Exp 2 and Exp 1. (a) 300hPa; (b) 850hPa. Dashed lines represent negative values, and solid lines positive values.

eastern Asia and Japan.This is resemblance to EUP(Eurasia-Pacific) teleconnection pattern. Over the tropical area to the south of the negative difference field region over southern Europe and Mediterranean, however, the difference region is positive. Comparing with the typical EUP pattern, one can find that the negative difference center over Europe is further south. The simulated results are consistent with those in Shukla and Wallace (1981), and are basically identical to observations in January, 1983 (Ouiroz, 1983). In southern upper troposphere, there also exist two different wave trains. One crosses central equatorial Pacific southeastward to the southern edge of south America, then returns to northeast and propagates into Atlantic and Africa. It consists of five difference centers with positive and negative one after another. The other starts from tropical African continent southeastward to southern Indian Ocean and finally enters southern Pacific and central-eastern equatorial Pacific associated with wavenumber 4.

The above results clearly indicate that because SSTA over central-eastern Pacific and the structure of zonal flow are unfavorable for the atmosphere to gain eddy kinetic energy (see Section V), the thermal source region in central Pacific turns to be the source of PNA-like wave train in the Northern Hemisphere and the eastern wave trains in the Southern Hemisphere, but the sources of wave trains similar to EUP-like in the Northern Hemisphere and the other wave trains in the Southen Hemisphere are located in tropical Indian Ocean and tropical Africa. Apparently, the formation of the latter is due to the influence of the SSTA over central-eastern Pacific on the equatorial east-west circulation, which intensifies the anomaly of convective heating over tropical Indian Ocean and tropical Africa. This assumption will be further verified in the next section.

Comparing Fig. 1a with Fig. 1b, we can find in upper and lower troposphere between 30°S—30°N that, the phases of the eddies are the same, and the positions of the eddy centers are close to each other, but the region of eddy center in the lower troposphere contrasting to that in the upper is near the equator. These results reflect that the vertical structure of eddy is baroclinic, and equivalent barotropic over the regions far away from equator.

2. *Difference Flow Field*

Figs. 2a and 2b give the difference flow field at 300hPa and 850 hPa.

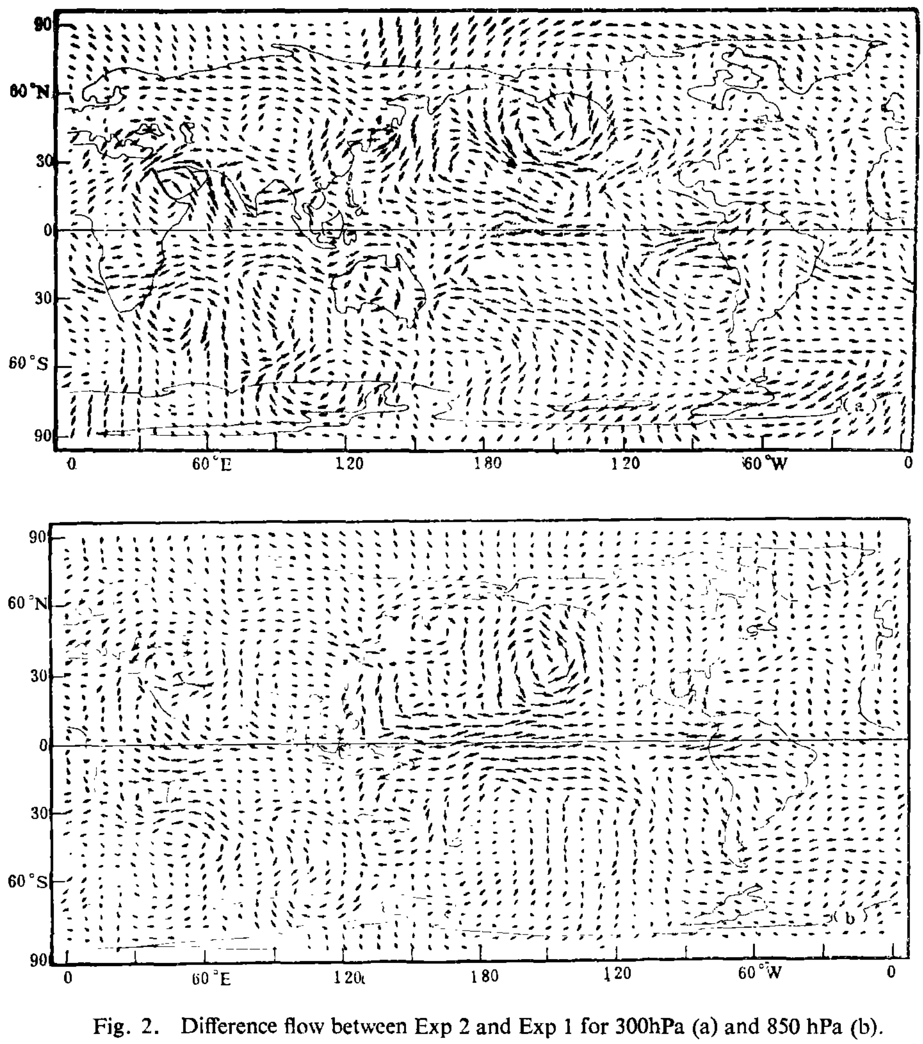

Fig. 2. Difference flow between Exp 2 and Exp 1 for 300hPa (a) and 850 hPa (b).

From Figs. 2a and 2b we can see that over the heat source in central-eastern equatorial Pacific, the 300hPa flow along equator is divergent; over east of the source region, it is westerly difference flow; over west side there exists easterly difference flow. However, over western equatorial Pacific it is convergent flow along the equator. It is easterly difference flow over the area east of 140°E, and westerly west of 140°E and east of 60°E. At 850hPa, It is convergent flow over the source with difference easterly over east side of the source and difference westerly over west side. There is devergent flow over equatorial western Pacific with westerly difference flow over the area east of 130°E and easterly west of 130°E. The distribution of difference flow and divergent and convergent regions in upper-lower layers described above is just opposite to the direction of equatorial Walker cell. As a result, it weakens the intensity of equatorial

Walker cell and east-west circulation over equatorial Indian Ocean associated with convergence in the upper and divergence in the lower over equatorial central-western Indian Ocean. At the same time, divergence in the upper and convergence in the lower exist over equatorial central Africa, resulting in reinforcing convective activity and forming new heat source over equatorial central Africa.

From Fig. 2a, it is further seen that the distribution of disturbance centers corresponding to difference regions in the geopotential height difference field is similar to the PNA pattern and EUP pattern in the Northern Hemisphere, whereas the counterpart of two wave trains in the difference flow field and the geopotential height field also exists in the Southern Hemisphere. There are a pair of anticyclonic difference circulations in the upper and a pair of cyclonic difference circulations in the lower over both sides of the equator to the west of the equatorial source. These simulated results are in agreement with theoretical results (Gill, 1980; Lau and Lim, 1984). The difference flow in the lower troposphere (Fig. 2b) shows that the phases and positions of difference circulations are consistent with those in the upper except for the regions near the equator while downstream of difference flow in the lower is opposite to that in the upper over the regions near the equator. These simulations agree with the response of simulated geopotential heights.

3. *Temperature Difference Field*

From the map of temperature difference field in the lower troposphere (Fig. 3b), it is seen that temperature increasing regions cover the whole Eurasian area except for polar regions of Asia and Europe, Southeast Asia and Mediterranean. In addition, there is an increase region of temperature over North America except for a few local regions, especially a warmer winter appears in north of North America. This simulated result is consistent with observations in December, 1982—Feb., 1983 (Quiroz, 1983). The temperature increasing area exists over central-eastern Pacific between 45°N and 45°S, which is in agreement with observations (Shukla and Wallace, 1983). There are temperature decreasing regions over higher latitudes, western Pacific and east of Indian Ocean while west of Indian Ocean is an increasing area. Variations of temperature are not apparent in the Atlantic Ocean.

Local difference between characteristics of temperature difference fields in the upper and in the lower is significant although they have several common characters. There exist increase regions over Pacific area except for high latitudes and equatorial western Pacific. There is a decrease area over the Indian Ocean except for equatorial Indian Ocean and a few regions in the Southern Hemisphere. Distribution of temperature in the Atlantic is reverse to that in the Pacific, where increase areas exist over higher latitudes and decrease areas over lower latitudes, with an exception that distribution in equatorial Atlantic is consistent with that in equatorial Pacific. Decrease regions of temperature appear to be over Europe and the south of Asia and increase regions over middle-high latitudes of Asia (except for the polar area) and North America.

According to the above simulation, it is clearly seen that El Nino has a different influence on temperature of the troposphere. It is higher over north of the continents and lower over south of the continents and vice versa over oceans. The most apparent influence areas are located in the Pacific, Indian Ocean, Eurasian continent and North American continents.

4. *Precipitation Difference Field*

Fig. 4 gives precipitation difference between Exp2 and Exp1. Fig. 4 clearly shows that

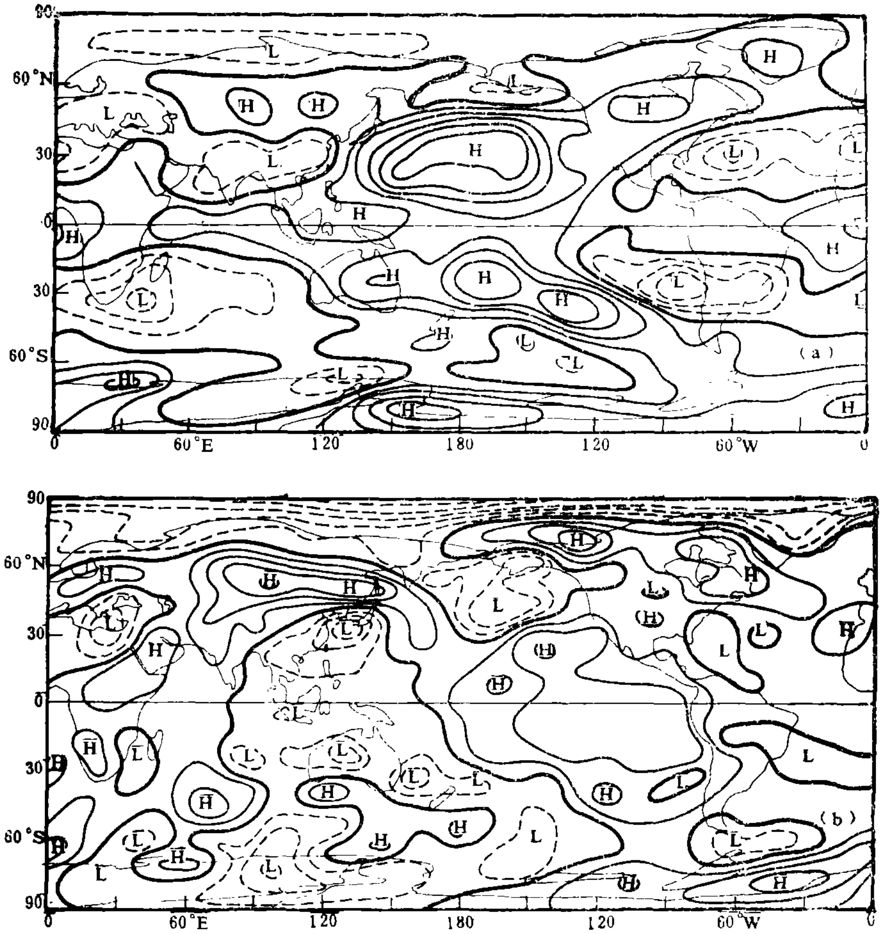

Fig. 3. Temperature difference field between Exp 2 and Exp 1 for 300hPa(a) and 850 hPa (b). Interval: 1.2°C.

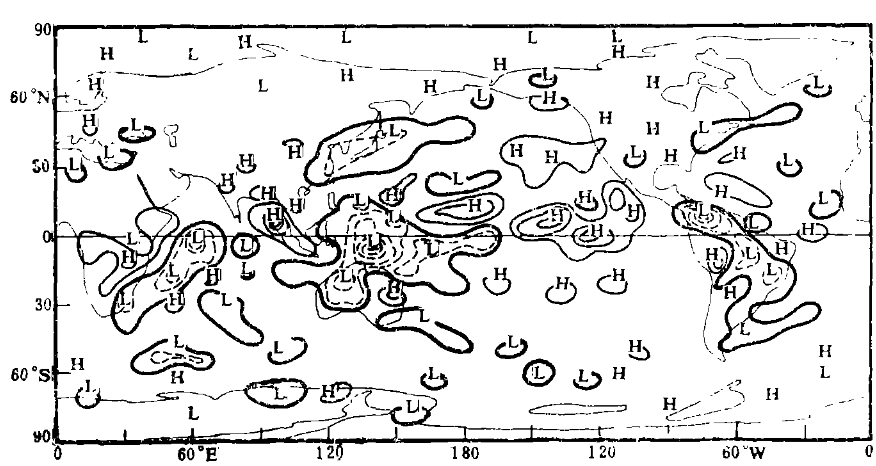

Fig. 4. Precipitation difference map between Exp 2 and Exp 1. Interval: 1 mm/day; dashed lines represent positive values; solid lines negative values.

there are increase regions of precipitation in equatorial central-eastern Pacific and equatorial central Africa, reflecting enhancement of convective activities.However, precipitation decreases in equatorial western Pacific and equatorial Indian Ocean near 60°E. The character of precipitation distribution that precipitation decreases in west of equatorial Pacific and increases in east of it, is similar to the observed character in the El Nino year (Shukla and Wallace 1983), and also consistent with weakening of equatorial east-west circulation. There exist increase regions of precipitation in south of Asia whereas decrease regions of precipitation in South China, part of Northeast China, and Japan. Precipitation increases are found in the west coast and northeast coast of South America, and south of Africa except for southeast coast areas while precipitation decreases in north of Africa and other areas.

The above distribution of simulated precipitation is in basical agreement with observed precipitation anomalies in winter during the El Nino period of 1982—1983 (Bergman et al., 1985). The fact described above reflects that main characters of precipitation distribution during the El Nino period are basically simulated.

IV. DYNAMICAL CHARACTERISTICS AND HORIZONTAL STRUCTURE OF THERMALLY FORCED SHORT-TERM CLIMATIC OSCILLATIONS IN NORTHERN WINTER

In this paper, the normal mode technique is used to decompose the simulated results in order to investigate dynamical characteristics of short-term climatic oscillations. The normal mode method was described in detail by Ni and Lin (1990).

In the normal mode technique, $J+1$ eastward and westward propagating gravity waves and westward propagating Rossby waves are respectively obtained for each vertical mode and wavenumber (except for wavenumber zero). Furthermore, their frequencies satisfy the following relation:

$$L(G_J^W)>\cdots>L(G_0^W)>L(R_0)>\cdots>L(R_J)>0>L(G_0^E)>\cdots>L(G_J^E).$$

Among them the characteristic wave with $L(G_0^E)$ refers to as Kelvin wave because its meridional perturbated velocity is very small. But the wave with $L(R_0)$ possesses character of Rossby-gravity mixed wave.

We make use of the normal modes described above to decompose the difference flow field between Exp 2 and Exp 1 in order to analyze characteristics and structure of the forced waves by SSTA over equatorial central-eastern Pacific.

Fig. 5a gives extralong wave component of Rossby mode at 300hPa. It shows that a pair of anticyclonic Rossby modes are formed on both sides of west of the heat source in the upper and a pair of cyclonic Rossby modes in the lower whereas on both sides of east of the heat source, a pair of cyclonic Rossby modes are formed in the upper and a pair of anticyclonic Rossby modes in the lower. Along the equator, there is difference easterly in the upper and difference westerly in the lower over east of the heat source and the reverse of this happens over the area east of 90°W; there is difference easterly in the upper and westerly in the lower over west of the heat source and the reverse of this happens further west of the source. Apparently, a pair of anticyclonic and cyclonic Rossby modes in the upper and the lower on both south and north sides of the equator can arise as a result of atmospheric Rossby baroclinic response to the heat source over west of the source. Over east of the heat source, the direction of difference flow along the equator is opposite to that of Walker cell, thus resulting in weakening Walker cell. In middle-high latitudes of Southern and Northern Hemispheres, phases of Rossby modes in the upper and in the lower are the same. In the Pacific and North America area of the

Northern Hemisphere, there exists extralong wave component of Rossby mode similar to the PNA pattern.The response is also evident in the Southern Hemisphere.There basically is correspondence between extralong wave components of Rossby modes in the difference flow field and in geopotential height difference field, reflecting existence of apparent Rossby wave trains.

Fig. 5b gives long wave components (wavenumber 4—6) of Rossby mode. From Fig. 5b, it is clearly seen that long wave response of Rossby mode mainly exists in middle-high latitudes of Southern and Northen Hemispheres. Furthermore, it is more remarked in the Northern Hemisphere than that in the Southern Hemisphere and more remarked in the Eastern Hemisphere than in the Western Hemisphere. Comparing long wave components in the upper with those in the lower, it is also seen that long wave components of Rossby mode along middle-high latitudinal circle form a series of alternating cyclonic and anticyclonic disturbances with same phase in the vertical, namely equivalent barotropic structure. It is noteworthy that the response is the most evident in the Pacific and Indian Ocean areas whereas it is comparatively weak in the Atlantic area.

Of the above, an extralong wave train of Rossby mode and a long wave train of Rossby mode along a latitudinal circle in Southern and Northern Hemispheres can arise as a result of long wave and extralong wave component response of Rossby mode to equatorial SSTA. This result is consistent with the theoretical result of Lim and Chang (1983).

Comparing Fig. 5a with extralong and long wave composite map of Rossby mode (Fig. 5c) shows that positions and phases of extralong wave component of PNA-like Rossby mode are consistent with the PNA pattern in the composite map. This result clearly shows that the PNA pattern formed by forcing of the heat source in Figs. 5c and 1a mainly results from response of extralong wave component of Rossby mode. Furthermore, the location of anticyclonic and cyclonic difference centers across Eurasian continent in Fig. 5c corresponds to that of EUP-like geopotential height difference centers. Comparing Fig. 5c with Fig. 5a indicates that there exists apparent anticyclonic Rossby mode response in Fig. 5c whereas in Fig 5a, there is a cyclonic difference circulation, and there no longer exists apparent extralong wave response of Rossby mode over the area west of the above cyclonic difference circulation. Comparison of Fig. 5c with Fig. 5b shows that long wave component response of Rossby mode between 30°N and 60°N is well corresponding to EUP-like distribution in Fig. 5c and long wave component response of Rossby mode in the area between 90°W and 180°W and between 30°N and 60°N is consistent with phases of members of PNA-like in Fig. 5c. These results clearly suggest that the PNA-like response to SSTA over equatorial central-eastern Pacific results from extralong and long wave component responses of Rossby mode and the EUP-like response in Eurasian continent results from only long wave response of Rossby mode. From Figs. 5c and 5b, it is also seen that long wave response of Rossby mode mainly has an influence on members of the wave train in the Indean Ocean area of the Southern Hemisphere whereas the wave train in the Pacific and Atlantic areas mainly results from extralong wave response of Rossby mode.

Figs. 6a and 6b represent extralong wave response of Kelvin mode at 300hPa and 850 hPa, respectively. It is shown that there exist difference easterly in the upper and differnce westerly in the lower over the west of the heat source and a difference wind reversal is observed over the east of the source. These facts apparently reflect the existence of convergence in the lower of the heat source and divergence in the upper in association with ascending difference flow. This distribution of equatorial east-west zonal difference flow is just opposite to the direction of Walker cell. Evidently, extralong wave component response of Kelvin

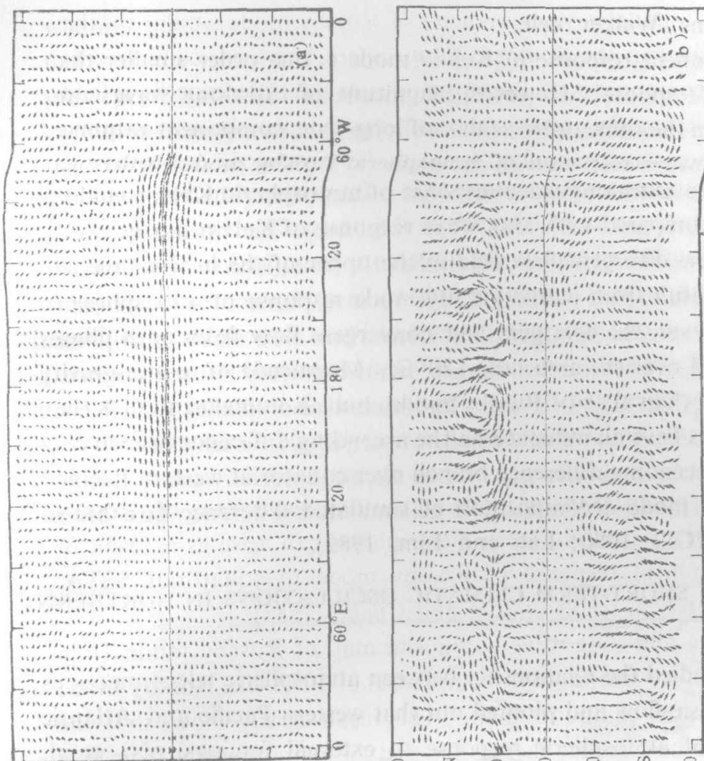

Fig. 6. Extralong wave components of Kelvin mode of difference flow for (a) 300 hPa and (b) 850 hPa.

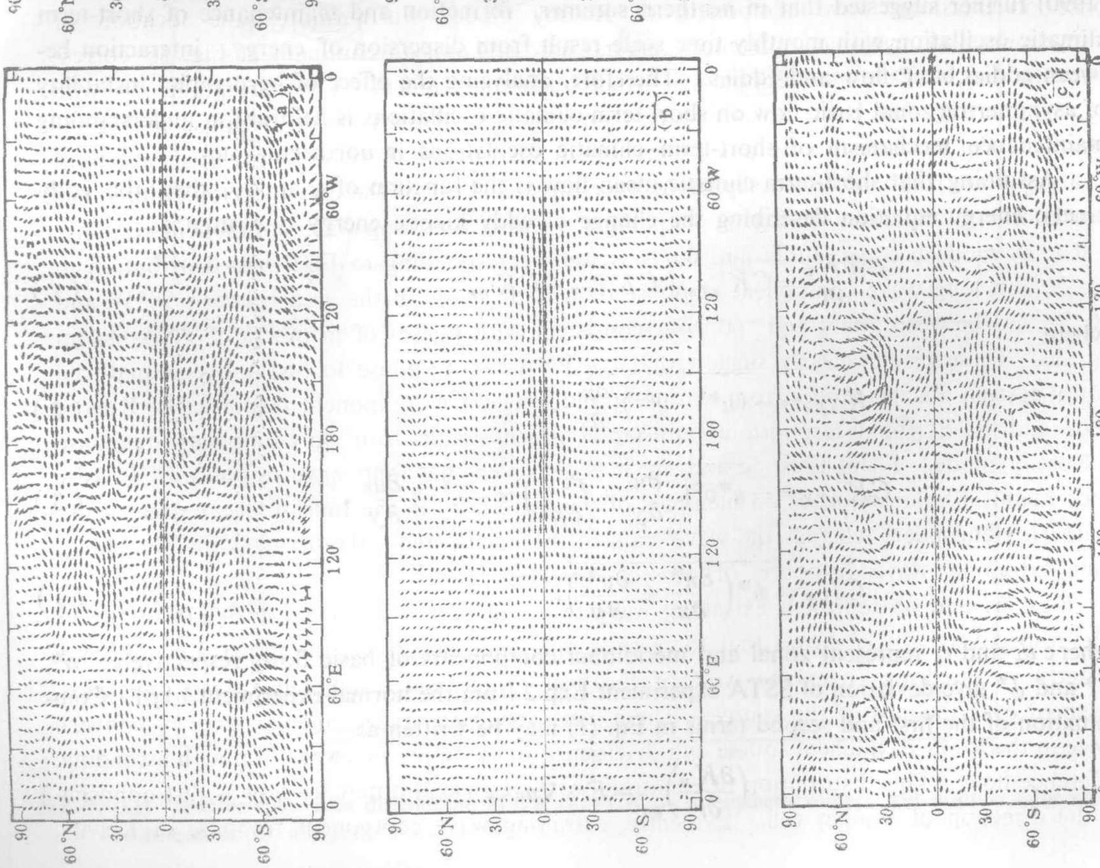

Fig. 5. (left panel) Rossby modes of 300 Pa difference flow for (a) extralong wave component (wavenumbers 1—3), (b) long component (wavenumbers 4—6) and (c) composite difference field

mode to the heat source weakens Walker cell.

Magnitude of long wave component response of Kelvin mode is one order smaller than that of extralong wave component response. However, magnitude of extralong wave component response of Rossby mode is in the same order as that of long wave component response. Therefore, extralong wave and long wave responses of atmospheric Rossby mode to the heat source are equally important whereas extralong wave response of atmospheric Kelvin mode to the heat source is more important compared with long wave response of Kelvin mode.

Finally, it is pointed out that the divergent flow field in the upper of the heat source and convergent flow field in the lower result from inertia-gravity mode response of atmosphere to the heat source (not shown). However, the divergent and convergent flow fields with phases reverse to the above flow are formed over the area near 120°E. Magnitude of inertia-gravity mode is not only one order smaller than that of Rossby mode, but also smaller than Kelvin mode. The above flow distributions have an influence on the ascending difference branch over equatorial eastern Pacific and the descending difference branch over equatorial western Pacific.

The above results from normal mode decomposition of simulated difference flow are in agreement with theoretical results (Gill, 1980; Lau and Lim, 1983).

V. MAINTENANCE MECHANISM OF SHORT-TERM CLIMATIC OSCILLATIONS IN NORTHERN WINTER

Simmons et al. (1983) have studied the relationship between atmospheric teleconnections and barotropic instable modes of basic flow and pionted out that western Pacific and Atlantic Ocean areas are sensitive regions of atmospheric response to external forcings. Ni et al. (1990) further suggested that in northern summer, formation and maintenance of short-term climatic oscillation with monthly time scale result from dispersion of energy, interaction between eddies,basic flow and eddies. Therefore, analyzing the effect of barotropic instability of asymmertric zonal basic flow on short-term climatic oscillations is helpful for understanding maintenance mechanism of short-term climatic oscillations in northern winter.

Assuming that short-term climatic mean flow is the function of x and y, then the eddy kinetic energy equation describing the change of eddy kinetic energy is written as

$$\frac{\partial K_E}{\partial t}=CK_{BTx}+CK_{BTy}+CK_p, \tag{1}$$

where

$$CK_{BTx}=-\overline{(u^{*2}-v^{*2})\frac{\partial u_b}{\partial x}}, \tag{2}$$

$$CK_{BTy}=-\overline{u^*v^*\left(\frac{\partial u_b}{\partial y}+\frac{\partial v_b}{\partial x}\right)}\simeq-\overline{u^*v^*\frac{\partial u_b}{\partial y}}, \tag{3}$$

$$CK_p=\overline{\phi^*\left(\frac{\partial u^*}{\partial x}+\frac{\partial v^*}{\partial y}\right)}, \tag{4}$$

where u_b and v_b represent zonal and meridional components of basic flow, respectively; u^*, v^* and ϕ^* give deviation of SSTA experiment Exp 2 from the normal experiment Exp1. Combination of the first and second terms in Eq. (1) may be written as

$$\left(\frac{\partial K_E}{\partial t}\right)_{BT}=\overline{E\cdot\nabla u_b}\ , \tag{5}$$

where

$$E = -(u^{*2} - v^{*2},\ u^{*}v^{*}),\qquad (6)$$

and represents zonal component of EP flux, which is an effective diagnostic available for studying interaction between zonal flow and transient eddies (Hoskins et al., 1983).

The first term in Eq. (1) reflects magnitude of interaction between zonal instablity of basic flow and zonal eddy momentum transport. Eddy kinetic energy increases in the regions where there exist zonally enlonged eddy ($u^{*2}>v^{*2}$) and $\partial u_b/\partial x<0$ or meridionally enlonged eddy ($v^{*2}>u^{*2}$) and $\partial u_b/\partial x>0$. It reflects the unstable effect of zonal asymmetric component of basic flow.The second term of Eq. (1) shows magnitude of interaction between meridional instability of basic flow and meridional transport of zonal momentum. It parallels to kinetic energy conversion between zonal symmetric basic flow ($\partial u_b/\partial x=0$) and eddies. The third term of Eq. (1) gives conversion of eddy potential energy to eddy kinetic energy.

Distribution of CK_{BTx} in northern winter of the El Nino year (not shown) shows that maximum areas of zonal kinetic energy conversion to eddy kinetic energy are located in northern Pacific, east of North America and east of North Africa, which result from unstable zonal

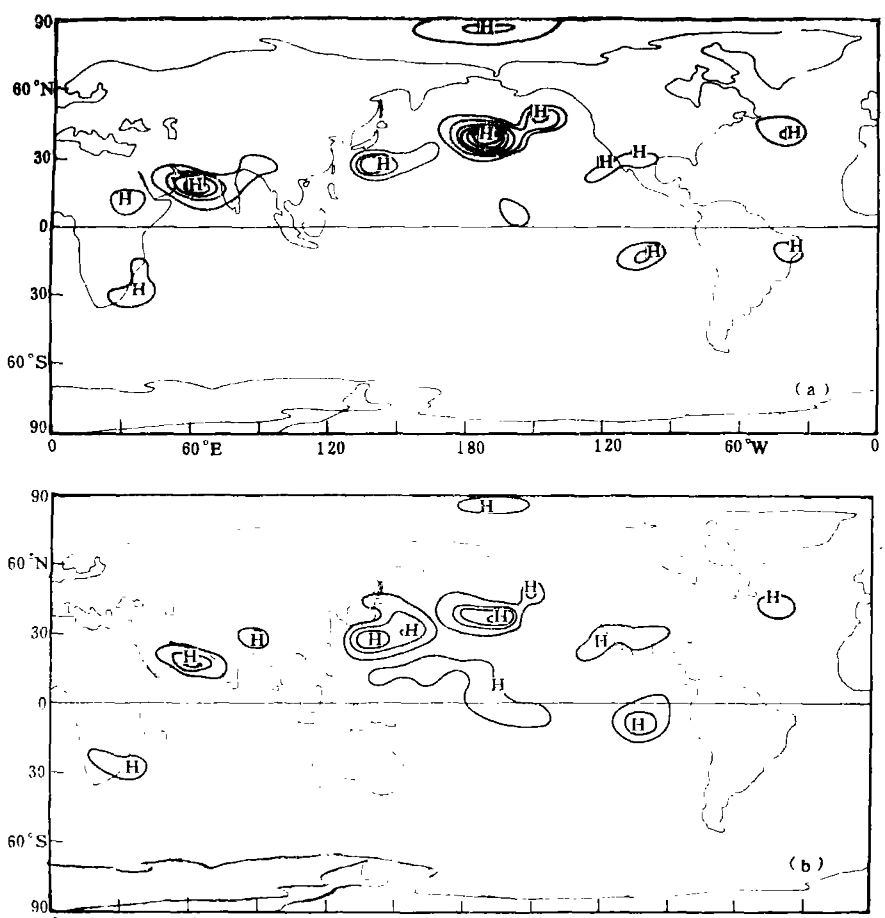

Fig. 7. (a) positive value area distribution of $CK_{BTx}+CK_{BTy}$ in northern winter; (b) positive value area distribution of CK_p.

asymmetric component. According to the above analysis, these are areas where there exist zonally enlonged eddy and $\partial u_b/\partial x<0$ or meridionally enlonged eddy and $\partial u_b/\partial x>0$. It is noteworthy that atmosphere over east and west of the heat source gains eddy kinetic energy in equatorial central Pacific.

Distribution map of CK_{BTy} (not shown) shows that there are three maximum regions of increase of eddy kinetic energy in northern Pacific. They are situated in southeast of extrance of both northern and western Pacific jets, respectively. The other two large value regions of increase of eddy kinetic energy are located in westerly jet extrance of eastern Northern America and south side of westerly jet over east of North Africa. The above results suggest that the most unstable region of basic flow is maximum eddy kinetic energy conversion region from zonal kinetic energy.

Distribution of $CK_{BTx}+CK_{BTy}$ (Fig. 7a) clearly shows that barotropic conversion of zonal kinetic energy to eddy kinetic energy mainly takes place in jet extrance over western Pacific and North America and the area where is maximum gradient of wind velocity over northern Pacific and east of north Africa.

Barotropic conversion of eddy kinetic energy in the Southern Hemisphere is smaller than that in the Northern Hemisphere. It is located in the jet extrance areas and large gradient areas of wind velocity, which is similar to that in the Northern Hemisphere.

Eddy potential energy conversion to eddy kinetic energy mainly takes place in eastern Pacific, northwestern Pacific, east of Asian continent, east of North Africa, equatorial western Pacific and Indian Ocean. In the Southern Hemisphere, eddy potential energy conversion to eddy kinetic energy is comparatively small, with its distribution corresponding to position of eddies. In comparison of the third term of Eq. (1) with the first and second terms, their magnitude order is basically the same. Therefore, conversion of eddy potential energy to eddy kinetic energy is also one of the main energy sources for maintenance of short-term climatic oscillations in the Northern Hemisphere (see Fig. 7b).

The above results clearly suggest that in northern winter main energy sources maintaining short-term climatic oscillations are zonal kinetic and eddy potential energy even in the El Nino period. This implies that eddies gain eddy kinetic energy because of barotropic instability of basic flow and convergence and divergence of disturbed flow. As a result, eddy members of the wave train are developed and maintained. This result is consistent with the conclusion of Ni et al. (1990) who analyzed short-term climatic oscillations in northern summer during the El Nino period. Comparing distribution of eddy kinetic energy conversion in northern winter of the El Nino year with that in northern summer of the El Nino year, we have found that seasonal difference of eddy kinetic energy conversion distribution causes the formations of PNA pattern and EUP pattern in northern winter and the teleconnection pattern similar to that suggested by Nitta (1987) in northern summer. This fact shows that seasonal difference of short-term climatic oscillations can arise as a result of seasonal difference of basic flow.

VI. SUMMARY AND CONCLUSIONS

According to the above results, conclusions can be drawn as follows:

(1) In northern winter, there exist two wave trains in the Northern Hemisphere because of an influence of El Nino, and they respectively bear resemblance to the PNA and EUP patterns. In the Southern Hemisphere, there are also two wave trains. One of them propagates southeastward from equatorial central Pacific and enters the Atlantic Ocean and equatorial Africa, and the other propagates southeastward from equatorial Africa then across south

Pacific and enters equatorial central-eastern Pacific. Flow field,temperature field and precipitation are anomalously changed because of existence of the wave trains described as above.

(2) The PNA-like wave train forced by SSTA over equatorial central-eastern Pacific results from extralong wave and long wave component responses of Rossby mode whereas the EUP-like wave train over Eurasian continent can arise as a result of long component response of Rossby mode. In the Southern Hemisphere, there mainly is long wave response of Rossby mode over the Indian Ocean and extralong wave response of Rossby mode over the Pacific and Atlantic. Extralong wave response of Kelvin mode is one order larger than long wave response of Kelvin mode thus resulting in weakening of Walker cell. These results are in general agreement with the theoretical results of Gill (1980) and Lau and Lim (1983).

(3) In northern winter, the warm water region in equatorial central Pacific is the forcing source of forced wave train in Northern and Southern Hemispheres, which is not only related to the warm water region in equatorial central Pacific, but also dependent on the structure character of zonal flow. In the El Nino year, the forcing source area of wave trains in northern winter apparently differs from that in northern summer. But the latter is located in equatorial western Pacific.

(4) In northern winter, energy sources maintaining short-term climatic oscillations from interactions between eddies, zonal flow and eddies result in conversion of eddy potential energy and zonal kinetic energy to eddy kinetic energy. The maximum conversion regions of eddy kinetic energy are mainly located in jet extrances and the areas where velocity gradient is maximum and related to structure of zonal flow.

REFERENCES

Bergman, K. Rl. et al. (1982), The global climate system, world climate data programme, WMO, 51pp.

Branstator, G. (1985), Analysis of general circulation model sea surface temperature anomaly simulation using a linear model, Part I: forced solutions, *J. Atmos. Sci.*, **42**:2225–2241.

Geisler, J.E., Blackmon, M.L., Bates, G.T. and Munoz, S. (1985), Sensitivity of January climate response to the magnitude and position of equatorial Pacific sea surface temperature anomalies, *J. Atmos. Sci.*, **42**:1037–1049.

Gill, A.E. (1980), Some simple solutions for heat induced tropical circulation, *Quart. J. R. Met. Soc.*, **106**:447–462.

Held, I.M. and Kang J.S. (1987), Barotropic models of the extratropical response to El Nino, *J. Atmos. Sci.*, **44**:3576–3586.

Horel, J.D. and Wallace, J.M.(1981), Planetary scale atmospheric phenomena associated with the southern Oscillation, *Mon. Wea. Rev.*, **109**:813–829.

Hoskins, B.J. and Karoly, D. (1981), The steady linear response of a spherical atmospheres to thermal and orographic forcing, *J. Atmos. Sci.*, **38**:1179–1196.

Lau, K.M. and Lim, Rl. (1984), On the dynamics of equatorial forcing of climate teleconnections, *J. Atmos, Sci.*, **41**:161–176.

Lim, H. and Chang, C.P. (1986),Generation of internal- and external-mode motions from internal heating: effects of vertical shear and damping, *J. Atmos. Sci.*, **43**:948–957.

Lin Yunbi and Sun Li (1987), Response of the atmosphere to central eastern equatorial Pacific sea surface temperature anomalies in July, *Scientia Meteor. Sin.*, 1987, No. 2, 1–13 (in Chinese).

McAvaney, B.J., Bourke, W. and Puri, K. (1978), A global model for simulation of general circulation, *J. Atmos. Sci.*, **35**:1557–1583.

Ni Yunqi and Lin Wuyin (1990),A numerical study for short-range climatic oscillation with various time scales forced by El Nino during the northern summer, *Acta Meteor. Sin.*, **4**:305–324.

Ni Yunqi, Lin Wuyin and Li Yaodong (1990), Formation mechanism and propagation characteristics of the equatorial thermally-forced short-term climatic oscillation during the northern summer,*Acta Meteor. Sin.* **4**:1–17.

Palmer, T.N. and Mansfield, D.A. (1986), A study of wintertime circulation anomalies during past El Nino event, using a high resolution general circulation model. II: Variability of the seasonal mean response, *Quart.*

J. Roy. Meteor. Soc.,**112**:639—660.

Quiroz, R.S. (1983), The climate of the "El Nino" winter of 1982-83-a season of extraordinary climatic anomalies, *Mon. Wea. Rev.*, **111**: 1685—1706.

Simmons, A.J. et al. (1983), Barotropic wave propagation and instability, and atmospheric teleconnection patterns, *J. Atmos. Sci.*, **40**: 1363—1392.

Shukla, J. and Wallace, J.M. (1983), Numerical simulation of the atmospheric response to equatorial Pacific sea surface temperature anomalies, *J. Atmos. Sci.*, **40**: 1613—1630.